$\mathcal{PT}$-Symmetric Scattering in Flow Duct Acoustics

Yves Aurégan* and Vincent Pagneux†
Laboratoire d'Acoustique de l'Université du Maine, UMR CNRS 6613 Avenue O Messiaen, F-72085 LE MANS Cedex 9, France
(Received 23 January 2017; published 28 April 2017)

We show theoretically and experimentally that the propagation of an acoustic wave in an airflow duct going through a pair of diaphragms, with equivalent amounts of mean-flow-induced effective gain and loss, displays all the features of a parity-time ($\mathcal{PT}$) symmetric system. Using a scattering matrix formalism, we observe, experimentally, the properties which reflect the $\mathcal{PT}$ symmetry of the scattering acoustical system: the existence of spontaneous symmetry breaking with symmetry-broken pairs of scattering eigenstates showing amplification and reduction, and the existence of points with unidirectional invisibility.

DOI: 10.1103/PhysRevLett.118.174301

Hydrodynamic instability theory shows that flow can provide energy to small perturbations [1,2]. If, in addition, these perturbations are compressible, then both acoustic wave propagation and energy exchange with the flow are possible, leading, e.g., to the classical whistling phenomena [3–5]. Thus, in the particular case of flow duct acoustics, the wave can obviously be convected but it also experiences gain or loss of acoustic energy due to interactions with the flow inhomogeneities [6]. Consequently, propagation of acoustic waves in ducts with flow is a natural non-Hermitian system where loss and gain are available.

Non-Hermitian systems, where energy conservation is broken, lead to dynamics governed by evolution equations with non-normal operators, where surprising phenomena can appear due to huge non-normality especially close to exceptional points [7–9]. The particular case of $\mathcal{PT}$ symmetry, where gain and loss are delicately balanced, has attracted a lot of attention in the last two decades [10–19]. It opens the possibility to obtain purely real spectra from non-Hermitian Hamiltonians, as well as spontaneous symmetry breaking where real eigenvalues coalesce at an exceptional point to become a complex conjugate pair. From a scattering point of view, another type of spontaneous symmetry breaking for $\mathcal{PT}$-symmetric systems has been theoretically proposed [20]. It corresponds to the transition of norm-preserving scattering eigenstates, with unimodular eigenvalues, to symmetry broken pairs of amplified and lossy scattering eigenstates, with associated pairs of scattering eigenvalues with inverse moduli [20–24]. It is to be noticed that this type of symmetry breaking is still waiting to be observed experimentally [25,26].

Initiated in the domain of quantum mechanics, many works on $\mathcal{PT}$ symmetry have displayed several intriguing effects such as power oscillation [15,27–29], unidirectional transparency [30–32], a single-mode laser [33,34], spectral singularity and a coherent perfect absorber (CPA) laser [20,35–38] or enhanced sensitivity [39]. A majority of the studies has been conducted in optics with some attempts in acoustics where the difficulty to obtain gain has been recognized. Actually, while losses can be easily introduced [40,41], the gain for acoustic waves has until now been obtained owing to active electric amplification [42–45].

In this Letter, we report the experimental realization of a purely mechanical scattering $\mathcal{PT}$-symmetric system for the propagation of acoustic waves in a waveguide. The loss and the gain are produced by two localized scattering units made of diaphragms, one associated with loss and the other associated with gain, see Fig. 1(a). In our experiments, the Mach number of the flow is small enough ($\mathrm{Ma} \simeq 0.01$) such that the effect of convection on the sound wave can be neglected, preserving the reciprocity property, and the only effect of the flow is located at the two diaphragms, characterized by normalized complex impedances C_1 and C_2. Note that, for a larger Mach number, an advected term in the Helmholtz equation would lead to a generalized $\mathcal{PT}$-symmetric system [46] that would be nonreciprocal. The balance of gain and loss is realized by finely tuning the flow rate and the geometry of each diaphragm, ensuring

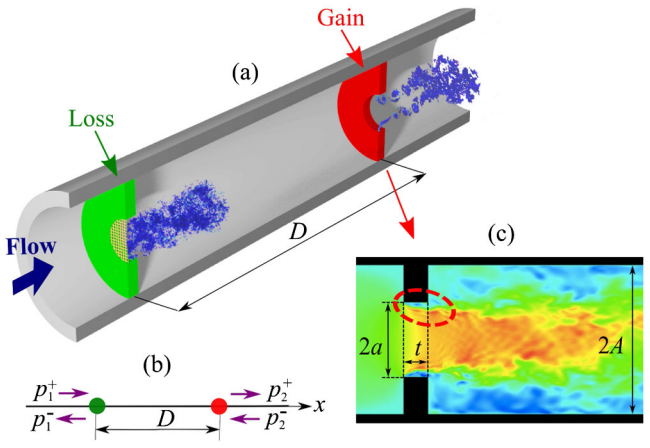

FIG. 1. (a) Sketch of the acoustic $\mathcal{PT}$-symmetric system in an airflow duct. (b) Corresponding 1D model. (c) Numerical simulation with Large Eddies Simulation [47] of the flow in the diaphragm in the presence of an acoustic wave.

a $\mathcal{PT}$-symmetric system that corresponds to $C_1 = C_2^*$ (note that the real part of the two normalized impedances have to be equal to get the parity symmetry). Measurements of the scattering matrix components allow us to demonstrate unidirectional invisibility and to verify the $\mathcal{PT}$-symmetry properties. Besides, by changing the distance between the scatterers, the spontaneous symmetry breaking of the scattering matrix is observed with the transition from exact-$\mathcal{PT}$-symmetric phase to $\mathcal{PT}$-broken phase. In the broken phase, with the experimental gain available, the scattering eigenstates can be simultaneously fourfold amplified or reduced, and we show that this effect might be enhanced by considering a finite periodic collection of the set of two diaphragms, leading to CPA-laser points.

System description and 1D model.—The description of the setup is shown in Fig. 1. We consider an acoustic waveguide where only plane waves can propagate ($kA < 1.841$ [48], where A is the tube radius, $k = \omega/c_0$ is the wave number, ω is the frequency and c_0 is the sound velocity). The propagation for the acoustic pressure p is then governed by the 1D Helmholtz equation. Two diaphragms are inserted into the tube and are separated with a distance D [Fig. 1(a)]. As their thicknesses t are small ($kt \ll 1$), the acoustic velocity is conserved while the pressure jumps between the two sides of the discontinuities. Thus the propagation is governed by

$$p'' + k^2 p = 0, \tag{1}$$

with the point scatterer jump conditions at the diaphragms:

$$[p']_{x=\pm D/2} = 0,$$
$$[p]_{x=-D/2} = \frac{C_1}{k} p', \quad \text{and} \quad [p]_{x=D/2} = \frac{C_2}{k} p',$$

where prime is the derivative with respect to x. The real part of the dimensionless parameters $C_{1,2}$ (that are acoustical impedances divided by the characteristic impedance and multiplied by i) is associated with reactive effects while its imaginary part is linked to the dissipative or gain effects. We have thus a very simple 1D reciprocal wave model with two point scatterers at $x = \pm D/2$ [Fig. 1(b)]. The effect of the flow on acoustic propagation is only and entirely contained in the normalized impedances C_1 and C_2 that reflect the mean-flow-induced effective gain and loss.

The system is $\mathcal{PT}$ symmetric if and only if the two normalized impedances are complex conjugated: $C_2 = C_1^*$ [49]. With the $\exp(-i\omega t)$ convention, there is absorption if $\Im(C_i) > 0$ and gain if $\Im(C_i) < 0$. The overall behavior of the acoustical system can be described by the transfer matrix M

$$\begin{pmatrix} p_2^+ \\ p_2^- \end{pmatrix} = \begin{bmatrix} M_{11} & M_{12} \\ M_{21} & M_{22} \end{bmatrix} \begin{pmatrix} p_1^+ \\ p_1^- \end{pmatrix} \tag{2}$$

where $p_{1,2}^+$ and $p_{1,2}^-$ are defined in Fig. 1(b). After some algebra, the components of the overall transmission matrix are found to be

$$M_{11} = -i\sin(kD)\frac{C_1C_2}{2} + e^{ikD}\left(1 + \frac{iC_1}{2} + \frac{iC_2}{2}\right),$$
$$M_{12} = i\sin(kD)\frac{C_1C_2}{2} - e^{ikD}\frac{iC_1}{2} - e^{-ikD}\frac{iC_2}{2},$$
$$M_{21} = -i\sin(kD)\frac{C_1C_2}{2} + e^{-ikD}\frac{iC_1}{2} + e^{ikD}\frac{iC_2}{2},$$
$$M_{22} = i\sin(kD)\frac{C_1C_2}{2} + e^{-ikD}\left(1 - \frac{iC_1}{2} - \frac{iC_2}{2}\right), \tag{3}$$

where in the case of a $\mathcal{PT}$-symmetric system [21] $M_{11} = M_{22}^*$ and $\Re[M_{12}] = \Re[M_{21}] = 0$. The transmission and reflection coefficients for waves coming from left and right are defined by $t_L = \det(\mathsf{M})/M_{22}$, $r_R = M_{12}/M_{22}$, $r_L = -M_{21}/M_{22}$, $t_R = 1/M_{22}$. Because of reciprocity we have $\det(\mathsf{M}) = 1$ and then $t = t_L = t_R$. As discussed in detail in Ref. [21], by permutation of the outgoing waves, two different scattering matrices with different sets of eigenvalues can be defined, leading to distinct symmetry breaking. These two scattering matrices are

$$\mathsf{S}_r = \begin{bmatrix} r_L & t \\ t & r_R \end{bmatrix} \quad \text{and} \quad \mathsf{S}_t = \begin{bmatrix} t & r_L \\ r_R & t \end{bmatrix}, \tag{4}$$

$$\text{where } \begin{pmatrix} p_1^- \\ p_2^+ \end{pmatrix} = \mathsf{S}_r \begin{pmatrix} p_1^+ \\ p_2^- \end{pmatrix}, \text{ and } \mathsf{S}_t = \mathsf{S}_r\sigma_x, \tag{5}$$

σ_x is one of the Pauli matrices. The eigenvalues of S_r and S_t may have both an exact and broken phases but the symmetry-breaking points are not the same. In this Letter, we have chosen to consider both S_r and S_t and the different phase transitions they imply. When computing the scattering eigenvalues, it is useful to recall the $\mathcal{PT}$-symmetry conservation relations [20,21,46,50] that can be written for instance as $\mathsf{S}_t^* = \mathsf{S}_t^{-1}$ and lead to

$$r_L^* r_R = 1 - |t|^2, \tag{6}$$

$$r_L t^* + r_L^* t = 0, \tag{7}$$

$$r_R t^* + r_R^* t = 0. \tag{8}$$

The eigenvalues of the scattering matrix S_t are given by $\lambda_{1,2} = t \pm \sqrt{r_R r_L} = t(1 \pm \sqrt{1 - |t|^{-2}})$. Then if $|t| < 1$, the modulus of the eigenvalues is equal to 1. The case $|t| = 1$ corresponds to symmetry breaking and $|t| > 1$ correspond to the $\mathcal{PT}$-broken phase. The eigenvalues of the other scattering matrix S_r are given by $s_{1,2} = (r_R + r_L \pm \sqrt{\Delta})/2$ where $\Delta = (r_R - r_L)^2 + 4t^2$. The broken phase condition can be written $\Delta = 0$ which leads to $r_R - r_L = \pm 2it$. In

terms of the transmission matrix coefficients, it is equivalent to $M_{12} - M_{21} = \pm 2i$ or $\Im(C_1)\sin(kD) = \pm 1$.

Experimental setup.—As described in Fig. 1, the $\mathcal{PT}$-symmetric system is mounted in a rigid circular duct between two measurement sections, upstream and downstream. Each measurement section consists in a hard walled steel duct (diameter 30 mm) where two microphones are mounted. Two acoustic sources on both sides of the system give two different acoustic states and the four elements of the scattering matrix (transmission and reflection coefficient on both directions) for plane waves can be evaluated. A more detailed description of the measurement technique can be found in Ref. [51]. The desired gain scatterer is realized by a finely designed diaphragm submitted to a steady flow. In this geometry, a shear layer is formed on its upstream edge and the flow is contracted into a jet with an area smaller than the hole of the diaphragm, see Fig. 1(c). This shear layer is very sensitive to any perturbations, like an oscillation in the velocity due to the acoustic wave. The shear layer convects and amplifies these perturbations [see the marked zone in Fig. 1(c)] and a strong coupling between acoustic and flow occurs when the acoustical period is of the order of the time taken by the perturbations to go from the upstream edge of the diaphragm to the exit of the diaphragm. This corresponds to a Strouhal number of the order of $S_h = ft/U_d \sim 0.2$ [47,51] where f is the frequency of the acoustic perturbation, t is the thickness of the diaphragm, and U_d is the mean velocity in the diaphragm $U_d = U_0(A/a)^2$ with U_0 the mean velocity in the duct and a the radius of the diaphragm [Fig. 1(c)]. Eventually, this gain diaphragm has been chosen with an internal radius $a = 10$ mm and a thickness $t = 5$ mm (see Fig. 1 and the inset in Fig. 2). The other diaphragm, that has to be lossy, has been chosen with an internal radius $a = 12$ mm and a thickness $t = 4.3$ mm. Two resistive metallic tissues have been glued in the diaphragm to produce some local viscous dissipation along this very fine wire mesh.

In a first step, the scattering coefficients of the two diaphragms have been measured separately, allowing us to deduce the values of the normalized impedance $C_{1,2}$. These parameters, that have to verify $C_2 = C_1^*$ to get a $\mathcal{PT}$-symmetric system, are plotted on Fig. 2. With the chosen geometry and flow parameters, it can be observed that there is a frequency f_m where the desired equality ($C_2 = C_1^*$) is achieved. In a second step, the scattering matrix of the system composed by the two balanced diaphragms is measured. All the subsequently reported measurements are made at the frequency $f_m = 1920$ Hz and at the Mach number $\mathrm{Ma} = 0.01$ for which $C_2 = C_1^* = 1.83$–$1.36i$, allowing the system to be $\mathcal{PT}$ symmetric. In order to be able to observe the symmetry breaking, the distance between the two diaphragms D is varied from 312 mm to 417 mm by inserting 22 rigid metallic tubes of different lengths. The minimal distance is chosen to minimize the hydrodynamical interactions between the two diaphragms.

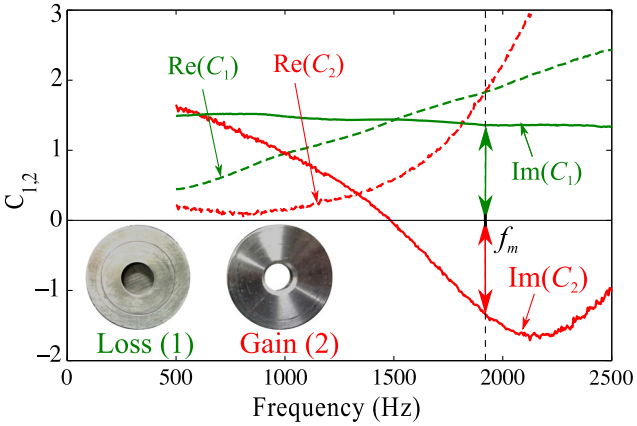

FIG. 2. Real and imaginary part of the measured impedance parameters C_1 and C_2. When the imaginary part of C_2 is negative the diaphragm gets some gain. At the frequency $f = f_m$, gain and loss are balanced $C_2 = C_1^*$.

The maximal D is chosen to have points over half a wavelength at the measurement frequency with a value of $kD/2\pi$ approximately in the range 1.7–2.4.

Results.—The measured transmission and reflection coefficients are displayed in Fig. 3(a). They are compared to the theoretical values obtained by using the measured value of $C_1 = C_2^*$ and the 1D modeling of Eqs. (3). The reflections from left r_L (impinging on the loss) and right r_R (impinging on the gain) appear as deeply asymmetric, with two points with $|t| = 1$ and $r_R = 0$ or $r_L = 0$. These two points correspond to the unidirectional transparency phenomenon where the wave passes unreflected with no amplitude change through the scatterers from one side, and is strongly reflected from the other side. In order to verify experimentally the $\mathcal{PT}$ symmetry of the system, in Fig. 3(b), we plot the 2-norm of the matrix $\mathsf{S}_t\mathsf{S}_t^* - \mathsf{I}$ corresponding to the shift from the $\mathcal{PT}$-symmetry conservation relations in Eqs. (6)–(8). For comparison, the norm of the matrix $\mathsf{S}_t{}^t\mathsf{S}_t^* - \mathsf{I}$ which represents the deviation to the acoustic energy conservation is also displayed. It appears that $\|\mathsf{S}_t\mathsf{S}_t^* - \mathsf{I}\|$ is nearly equal to zero in the whole

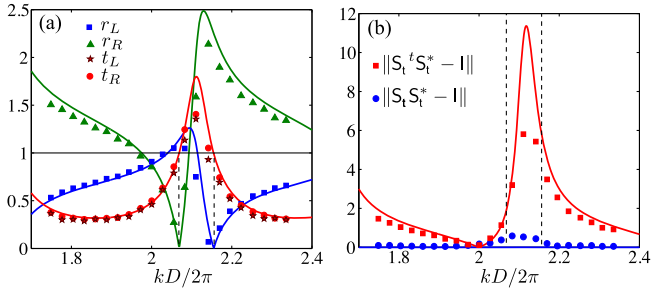

FIG. 3. (a) Modulus of the scattering coefficients. (b) Norm of the deviation from acoustic energy conservation property and from the $\mathcal{PT}$-symmetry property of the scattering matrix. Symbols correspond to experimental measurements and solid lines correspond to the 1D theory.

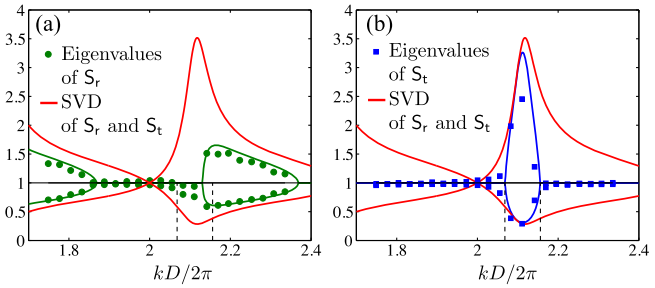

FIG. 4. Spontaneous symmetry breaking of the scattering matrices. (a) Green points: measurements, green line: 1D theory. (b) Blue points: measurements, blue line: 1D theory. In each plot, the red lines correspond to the two SVDs of the scattering matrix. Dashed lines correspond to $|t| = 1$, i.e., the phase transition for S_t.

range of paramaters which unambiguously demonstrates that the system is $\mathcal{PT}$ symmetric; meanwhile $\|\mathsf{S}_t{}^t\mathsf{S}_t^* - \mathsf{I}\|$ can take large values confirming that our system strongly violates conservation of acoustic energy because the mean flow can be seen as a supplier of energy for the acoustic wave. Note that the deviation from the $\mathcal{PT}$-symmetric conservation relation when kD is around 2.1 can be modeled by taking into account the viscothermal damping in the propagation between the two diaphragms [52]. It can be noticed that for the kD multiple of π, the system is simultaneously $\mathcal{PT}$ symmetric and conservative; it can be verified [see Eqs. (3)] that in these cases the scattering is only sensitive to the real part of the normalized impedances C_1 and C_2, ignoring thus the effect of gain and loss.

By varying the length of the duct between the two diaphragms, we can also inspect the spontaneous symmetry breaking of the scattering matrix of the system [20]. In Fig. 4, we show the eigenvalues of S_r and S_t that, since they are different, lead to different symmetric and broken phases [21]. We represent also the singular value decomposition (SVD) of the scattering matrices. These two SVDs are identical for S_t and S_r (since $\mathsf{S}_t{}^t\mathsf{S}_t^* = \mathsf{S}_r{}^t\mathsf{S}_r^*$) and correspond, respectively, to the maximum and minimum outgoing wave for any incoming waves with unit flux; by definition they are the upper and lower bound of the modulus of the eigenvalues, and thus must be different from one, to allow the broken phase. For each choice of scattering matrix, the experimental measurements, very close to the theoretical predictions, display clear signatures of the spontaneous symmetry breaking with different broken phases for S_t and S_r. In the symmetric phase the eigenvalues of the scattering matrices remain on the unit circle in the complex plane, and the symmetry breaking corresponds to pairs of non-unimodular scattering eigenvalues, i.e., where the moduli are the inverse of each other and different from 1. To the best of our knowledge, it is the first experimental demonstration of the symmetry breaking of the scattering matrix for $\mathcal{PT}$-symmetric systems as proposed in Ref. [20].

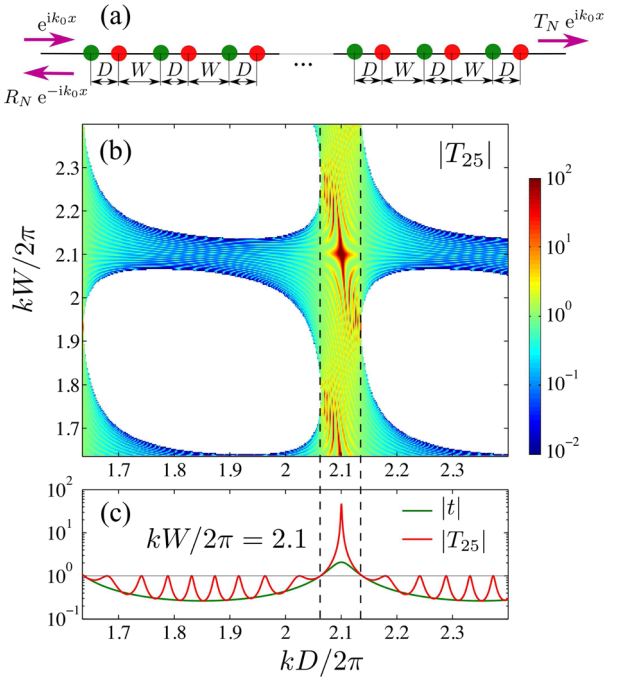

FIG. 5. (a) Finite periodic case with N cells, green (red) is a scatterer with loss (gain). (b) Transmission coefficient as a function of kD and kW for $N = 25$. White regions correspond to band gaps. (c) Transmission for $kW/2\pi = 2.1$.

In the broken phase, a particularly interesting case is the CPA laser where one eigenvalue of the S matrix goes to infinity (laser) and the other goes to zero (absorber). From the experimental results of Fig. 4 we can see that this laser absorber is not achieved because the maximum eigenvalue corresponds to a 3.5 amplification. From Eqs. (3), it can be shown that the CPA-laser condition can be obtained for larger values of the gain parameter ($\Im(C_2) \simeq 2.5$) which cannot be achieved with our current experimental setup. Nevertheless, in Fig. 5, we show that quasi-CPA laser could be theoretically achieved by taking a finite periodic array of N cells of our $\mathcal{PT}$-symmetric system with a distance W between each cell [Fig. 5(a)]. The use of the 1D model shows that quasi CPA laser can be obtained by just tuning the number of cells and the intercell dimensionless frequency kW [$N = 25$ and $kW/2\pi = 2.1$ in Figs. 5(b) and 5(c)]. Figure 5(c) indicates that, by using the interference Bragg effect in the finite periodic case, it is possible to approach, very closely, the conditions of the CPA laser.

Conclusion.—Owing to vortex-sound interaction providing gain and loss in an acoustical system, we have obtained the experimental signatures of the spontaneous $\mathcal{PT}$-symmetry breaking in scattering systems. The scattering matrix eigenvalues can remain on the unit circle in the complex plane despite the non-Hermiticity and the symmetry breaking results in pairs of scattering eigenvalues with inverse moduli. Unidirectional transparency has also been observed. It is noteworthy that this mechanical gain medium is not required to be electronically powered and

that this $\mathcal{PT}$-symmetric system is very simple to manufacture: one tube, two diaphragms, and a small flow inside the tube. Therefore, this kind of acoustic system can be seen as a building block to study wave propagation with more complex $\mathcal{PT}$ symmetry (for instance in periodic systems), and, more generally, we believe it provides an important connection between hydrodynamic instability theory, acoustic wave propagation, and non-Hermitian physics.

*yves.auregan@univ-lemans.fr
†vincent.pagneux@univ-lemans.fr

[1] P. J. Schmid and D. S. Henningson, *Stability and Transition in Shear Flows* (Springer Science & Business Media, New York, 2012), Vol. 142.
[2] P. G. Drazin and W. H. Reid, *Hydrodynamic Stability* (Cambridge University Press, Cambridge, England, 2004).
[3] W. Mohring, E. A. Muller, and F. Obermeier, Rev. Mod. Phys. **55**, 707 (1983).
[4] M. E. Goldstein, *Aeroacoustics* (McGraw-Hill International Book Co., New York, 1976).
[5] A. L. Fabrikant and Y. A. Stepanyants, *Propagation of Waves in Shear Flows* (World Scientific, Singapore, 1998), Vol. 18.
[6] M. S. Howe, J. Fluid Mech. **71**, 625 (1975).
[7] L. N. Trefethen and M. Embree, *Spectra and Pseudospectra: The Behavior of Nonnormal Matrices and Operators* (Princeton University Press, Princeton, NJ, 2005).
[8] N. Moiseyev, *Non-Hermitian Quantum Mechanics* (Cambridge University Press, Cambridge, England, 2011).
[9] D. Krejcirik, P. Siegl, M. Tater, and J. Viola, J. Math. Phys. **56**, 103513 (2015).
[10] C. M. Bender and S. Boettcher, Phys. Rev. Lett. **80**, 5243 (1998).
[11] A. Mostafazadeh, J. Math. Phys. (N.Y.) **43**, 205 (2002).
[12] C. M. Bender, Contemp. Phys. **46**, 277 (2005).
[13] C. M. Bender, Rep. Prog. Phys. **70**, 947 (2007).
[14] A. Guo, G. J. Salamo, D. Duchesne, R. Morandotti, M. Volatier-Ravat, V. Aimez, G. A. Siviloglou, and D. N. Christodoulides, Phys. Rev. Lett. **103**, 093902 (2009).
[15] C. E. Ruter, K. G. Makris, R. El-Ganainy, D. N. Christodoulides, M. Segev, and D. Kip, Nat. Phys. **6**, 192 (2010).
[16] R. El-Ganainy, K. G. Makris, D. N. Christodoulides, and Z. H. Musslimani, Opt. Lett. **32**, 2632 (2007).
[17] A. Regensburger, M.-A. Miri, C. Bersch, J. Nager, G. Onishchukov, D. N. Christodoulides, and U. Peschel, Phys. Rev. Lett. **110**, 223902 (2013).
[18] A. Cerjan, A. Raman, and S. Fan, Phys. Rev. Lett. **116**, 203902 (2016).
[19] Z. Zhang, Y. Zhang, J. Sheng, L. Yang, M.-A. Miri, D. N. Christodoulides, B. He, Y. Zhang, and M. Xiao, Phys. Rev. Lett. **117**, 123601 (2016).
[20] Y. D. Chong, L. Ge, and A. D. Stone, Phys. Rev. Lett. **106**, 093902 (2011).
[21] L. Ge, Y. D. Chong, and A. D. Stone, Phys. Rev. A **85**, 023802 (2012).
[22] P. Ambichl, K. G. Makris, L. Ge, Y. Chong, A. D. Stone, and S. Rotter, Phys. Rev. X **3**, 041030 (2013).
[23] P. A. Kalozoumis, G. Pappas, F. K. Diakonos, and P. Schmelcher, Phys. Rev. A **90**, 043809 (2014).
[24] B. Zhu, R. Lu, and S. Chen, Phys. Rev. A **93**, 032129 (2016).
[25] L. Ge, K. G. Makris, D. N. Christodoulides, and L. Feng, Phys. Rev. A **92**, 062135 (2015).
[26] L. Ge and L. Feng, Phys. Rev. A **94**, 043836 (2016).
[27] K. G. Makris, R. El-Ganainy, D. N. Christodoulides, and Z. H. Musslimani, Phys. Rev. Lett. **100**, 103904 (2008).
[28] A. Regensburger, C. Bersch, M.-A. Miri, G. Onishchukov, D. N. Christodoulides, and U. Peschel, Nature (London) **488**, 167 (2012).
[29] M. Kozlov and G. P. Tsironis, New J. Phys. **17**, 105004 (2015).
[30] Z. Lin, H. Ramezani, T. Eichelkraut, T. Kottos, H. Cao, and D. N. Christodoulides, Phys. Rev. Lett. **106**, 213901 (2011).
[31] S. Longhi, J. Phys. A **44**, 485302 (2011).
[32] S. Longhi, J. Phys. A **47**, 485302 (2014).
[33] L. Feng, Z. J. Wong, R.-M. Ma, Y. Wang, and X. Zhang, Science **346**, 972 (2014).
[34] H. Hodaei, M.-A. Miri, M. Heinrich, D. N. Christodoulides, and M. Khajavikhan, Science **346**, 975 (2014).
[35] A. Mostafazadeh, Phys. Rev. Lett. **102**, 220402 (2009).
[36] S. Longhi, Phys. Rev. A **82**, 031801(R) (2010).
[37] H. Ramezani, H. K. Li, Y. Wang, and X. Zhang, Phys. Rev. Lett. **113**, 263905 (2014).
[38] Z. J. Wong, Y.-L. Xu, J. Kim, K. OBrien, Y. Wang, L. Feng, and X. Zhang, Nat. Photonics **10**, 796 (2016).
[39] Z.-P. Liu, J. Zhang, S. K. Ozdemir, B. Peng, H. Jing, X.-Y. Lu, C.-W. Li, L. Yang, F. Nori, and Y.-X. Liu, Phys. Rev. Lett. **117**, 110802 (2016).
[40] V. Romero-Garcia, G. Theocharis, O. Richoux, A. Merkel, V. Tournat, and V. Pagneux, Sci. Rep. **6**, 19519 (2016).
[41] V. Romero-Garcia, G. Theocharis, O. Richoux, and V. Pagneux, J. Acoust. Soc. Am. **139**, 3395 (2016).
[42] R. Fleury, D. Sounals, and A. Alu, Nat. Commun. **6**, 5905 (2015).
[43] X. Zhu, H. Ramezani, C. Shi, J. Zhu, and X. Zhang, Phys. Rev. X **4**, 031042 (2014).
[44] C. Shi, M. Dubois, Y. Chen, L. Cheng, H. Ramezani, Y. Wang, and X. Zhang, Nat. Commun. **7**, 11110 (2016).
[45] J. Christensen, M. Willatzen, V. R. Velasco, and M.-H. Lu, Phys. Rev. Lett. **116**, 207601 (2016).
[46] H. Schomerus, Phil. Trans. R. Soc. A **371**, 20120194 (2013).
[47] R. Lacombe, S. Foller, G. Jasor, W. Polifke, Y. Aurégan, and P. Moussou, J. Sound Vib. **332**, 5059 (2013).
[48] A. D. Pierce, *Acoustics: An Introduction to its Physical Principles and Applications* (Acoustical Society of America, McGraw-Hill, New York, 1994).
[49] H. Mehri-Dehnavi, A. Mostafazadeh, and A. Batal, J. Phys. A **43**, 145301 (2010).
[50] A. Mostafazadeh, J. Phys. A **47**, 505303 (2014).
[51] P. Testud, Y. Aurégan, P. Moussou, and A. Hirschberg, J. Sound Vib. **325**, 769 (2009).
[52] See Supplemental Material at http://link.aps.org/supplemental/10.1103/PhysRevLett.118.174301 for an explanation of the deviation from the $\mathcal{PT}$-symmetry by the viscothermal effects.